4-16-2005

Spatial Variability in Biogenic Gas Accumulations in Peat Soils Is Revealed By Ground Penetrating Radar (GPR)

Xavier Comas

Lee Slater

Andrew S. Reeve
University of Maine - Main, asreeve@maine.edu

Spatial variability in biogenic gas accumulations in peat soils is revealed by ground penetrating radar (GPR)

Xavier Comas,[1] Lee Slater,[1] and Andrew Reeve[2]

Received 20 December 2004; revised 16 February 2005; accepted 15 March 2005; published 16 April 2005.

[1] We performed surface and borehole ground penetrating radar (GPR) tests, together with moisture probe measurements and direct gas sampling to detect areas of biogenic gas accumulation in a northern peatland. The main findings are: (1) shadow zones (signal scattering) observed in surface GPR correlate with areas of elevated CH_4 and CO_2 concentration; (2) high velocities in zero offset profiles and lower water content inferred from moisture probes correlate with surface GPR shadow zones; (3) zero offset profiles depict depth variable gas accumulation from 0–10% by volume; (4) strong reflectors may represent confining layers restricting upward gas migration. Our results have implications for defining the spatial distribution, volume and movement of biogenic gas in peatlands at multiple scales.
Citation: Comas, X., L. Slater, and A. Reeve (2005), Spatial variability in biogenic gas accumulations in peat soils is revealed by ground penetrating radar (GPR), *Geophys. Res. Lett.*, *32*, L08401, doi:10.1029/2004GL022297.

1. Introduction

[2] Peatlands emit significant amounts of CH_4 and CO_2 to the atmosphere [*Cicerone and Oremland*, 1988; *Rosenberry et al.*, 2003]. Although estimations of the total annual CH_4 flux to the atmosphere from northern peatlands are reported (e.g. approximately 7% [*Khalil*, 2000]), the effect of global warming on peatlands emissions is still a major uncertainty in climate modeling. Recent work suggests that the mass of free phase gas in peatlands is considerably greater than that in the dissolved phase [*Fechner-Levy and Hemond*, 1996]. Spatially and temporally variable ebullition fluxes may represent an important component of the free phase carbon gas release from peatlands to the atmosphere [*Romanowicz et al.*, 1995]. The dependence of CH_4 emissions on water table elevation [*Roulet et al.*, 1993], as well as the reduction in water flow due to pore space blocking by biogenic gas bubbles [*Beckwith and Baird*, 2001], indicate that hydrological processes regulate carbon cycling in peatlands. Unfortunately, the discontinuous pattern, as well as the phase instabilities, of gas bubbles in saturated porous media makes the measurement of free phase gas accumulation, its spatial distribution and temporal variation in peatlands difficult at the field scale.

[3] Investigation of free phase gas in peat has involved invasive sampling and subsequent laboratory measurements such as time domain reflectometry (TDR) [*Beckwith and Baird*, 2001], scanning electron microscopy [*Landva and Pheeney*, 1980] and magnetic resonance imaging [*Glaser et al.*, 1998]. Non-invasive efforts to estimate free gas phase volume and temporal gas release to the atmosphere in the field include (1) monitoring of water pressures in piezometers [*Rosenberry et al.*, 2003], and (2) monitoring of surface deformations associated with gas release using GPS [*Glaser et al.*, 2004], or aluminum elevation sensor rods [*Price*, 2003]. These methods have distinct limitations, e.g. disturbance of the natural distribution of gas within the peat during piezometer and rod installation, high measurement sensitivity required during GPS measurements and a limited support volume of the measurement.

[4] Ground penetrating radar (GPR) is widely used to evaluate water content in the vadose zone [e.g., *Huisman et al.*, 2003]. Zero offset profile (ZOP) measurements between boreholes can resolve 0.5% average moisture content variation [e.g., *Binley et al.*, 2001]. The surface reflection-mode GPR method shares many common characteristics with the seismic reflection method, widely used for mapping gas deposits contained in shallow marine sediments. Zones of faint or absent reflections (acoustic blanking) result from scattering of the acoustic energy in the presence of gas [e.g., *Judd and Hovland*, 1992]. Regions of gas accumulation can affect surface GPR in a similar manner. Previous GPR studies reveal regions of 'EM blanking' (scattering of EM energy) attributed to the displacement of water by hydrocarbon gas vapors [*Daniels et al.*, 1995; *Lopes de Castro and Branco*, 2003]. The aim of our study was to investigate the spatial distribution, gas content and volume of free phase biogenic gas within peatlands.

2. Experimental Design

[5] Surface and borehole GPR measurements were conducted at Caribou Bog, Maine. Moisture probe measurements and direct gas sampling were also performed. The study site (located 2 m from a pool) was chosen based on observations of significant gas release (ignitable with a match, confirming the presence of CH_4) during coring. Two 3″ diameter inclinometer casings were installed 5 m apart, from the surface to the top of the mineral soil (8.4 m) (h1 and h2 in Figure 1). ZOP surveys (250 MHz antenna frequency) were conducted to determine the travel time between borehole transmitter (h1) and borehole receiver (h2) as a function of depth in the peat. Surface GPR (100 MHz antenna) was also recorded along a profile joining the two inclinometer casings. Casing deviation from vertical was determined with an inclinometer survey.

[6] Water content estimates were collected between boreholes using a 0.2 m moisture probe (ECH_2O-20 dielectric aquameter, by Decagon) inserted by hand from the surface to depths close to the mineral soil. A total of nine lines separated by 0.5 m were recorded at 0.25 m depth intervals

[1]Department of Earth and Environmental Sciences, Rutgers University, Newark, New Jersey, USA.
[2]Department of Earth Sciences, University of Maine, Orono, Maine, USA.

0094-8276/05/2004GL022297

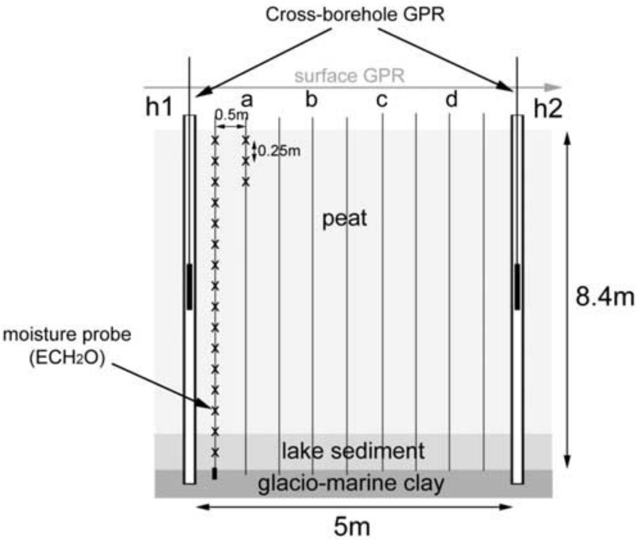

Figure 1. Instrumentation setup in the field between boreholes h1 and h2: surface GPR, borehole GPR, and moisture probe with a 1 m offset into the plane of image. Gas samples were collected along lines a, b, c, and d at locations determined by the surface GPR results. Lithological units inferred from direct sampling are also shown.

(Figure 1). The array was collected in a plane parallel to the GPR boreholes with a 1 m offset to prevent soil disturbance from affecting the ZOP GPR data.

[7] Free-phase gas samples were directly collected at selected depths based on the surface GPR results along lines a, b, c, and d (Figure 1). Samples were obtained using a Geoprobe rod gas sampling system, connected to a vacuum box containing 0.6 liter Tedlar sampling bags. Gas samples were transported to the laboratory and analyzed for CH_4 and CO_2 within 72 hours after collection with a Varian 3600 GC/FID/TCD gas chromatograph. Porosity was measured by oven drying eleven peat samples collected from the surface to the mineral soil in Caribou Bog. Dielectric permittivity measurements of three peat samples (0.5, 1.5, and 3 m depths) were taken in the laboratory using a high-resolution dielectric spectrometer (Novocontrol BDS-80).

3. Results

[8] A summary of the findings is presented in Figure 2. Although the GPR and moisture probe surveys were conducted to the top of the mineral soil (8.4 m), the results presented here are limited to the upper 6.5 m of good surface GPR signal recovery. The moisture probe results are expressed in terms of the absolute difference between probe output (in mV) at each depth and that at the surface. Variability in pore-water conductivity with depth, temperature change and the effect of overburden pressure prevented probe calibration for moisture content in the laboratory. Consequently, the moisture probe results only qualitatively represent moisture content, where more negative values are indicative of lower moisture content.

3.1. Shadow Zones and Gas Content

[9] Areas with higher concentration of CH_4 (up to 6,500 ppm of total gas present) and CO_2 (up to 5,000 ppm of total gas present) coincide with a shadow zone (EM blanking) apparent in the surface GPR profile (Figure 2b). This shadow zone is roughly defined as the region from 2.0–3.0 m between gas sampling lines b and d in Figure 2b. Two smaller localized shadow zones can be approximately defined in the surface GPR profile from 0.5–1.2 m and 3.4–4.2 m depth both between gas sampling lines b and d. An annotated sketch of the shadow zones is shown in Figure 2a. Areas with strong EM wave reflections (e.g. at approximately 4.5 m between gas sampling b and d) generally coincide with low gas concentrations. During installation of borehole h2, a sequence of underwater gas releases at different depths (red dots in Figure 2a indicate these depths) was recorded at the

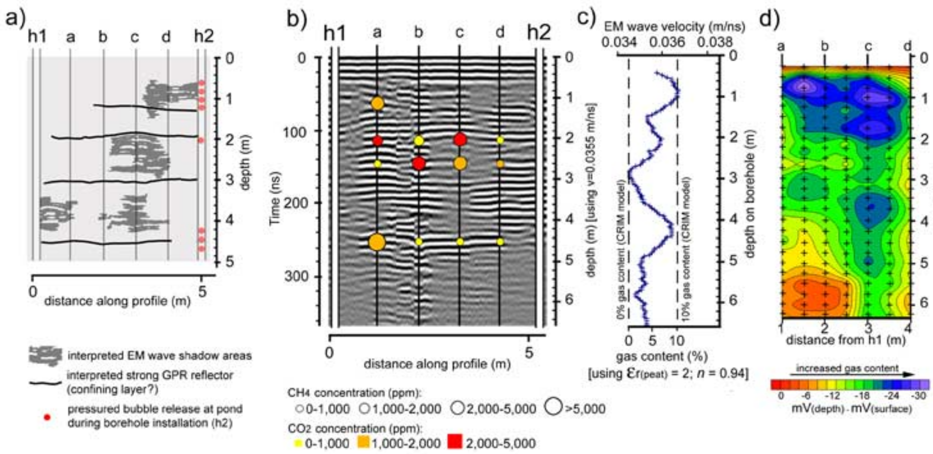

Figure 2. (a) Interpreted EM wave shadow areas and strong reflectors from surface GPR profile (Figure 2b). Depths of pressured bubble releases observed during borehole installation (h2) are also shown; (b) Surface GPR profile between the two boreholes (h1 and h2). Gas chromatography results for CH_4 and CO_2 gas sampling along four lines (a, b, c, and d) are also shown; (c) EM wave velocity obtained with borehole GPR, zero offset between transmitter (h1) and receiver (h2). Estimated maximum and minimum gas content (%) according to the CRIM model is also shown; (d) moisture probe measurements between line a and line d expressed as the absolute difference between mV output at each depth and the mV output at the surface.

pond situated next to the study area (parallel to and 2 m offset from plane h1-h2).

3.2. EM Wave Velocity Changes Between Boreholes

[10] Higher EM wave velocities computed from the travel time between borehole transmitter and borehole receiver generally coincide with the shadow zones observed in the surface GPR data and the higher biogenic gas concentrations recorded (Figure 2c). Three high EM wave velocity zones can be defined between 0.5–1.2 m, 1.8–2.5 m, and 3.8–4.4 m depth respectively (Figure 2c), correlating with the shadow zones as previously described, and the higher concentrations of gas extracted. The moisture probe measurements (Figure 2d) show two negative areas (lower mV reading as compared to the surface) between 0.5–2 m depth, and 3.5–5 m depth. Positive values (orange-red colored) are defined from 0.2–0.5 m depth, and from 5–6.2 m depth.

3.3. Gas Estimates Using the CRIM Model

[11] The Complex Refractive Index Model (CRIM) [e.g., *Huisman et al.*, 2003] expresses the bulk permittivity (ε_b) of a soil measured with TDR or GPR as:

$$\varepsilon_{r(b)} = \theta\varepsilon^{\alpha}_{r(w)} + (1-n)\varepsilon^{\alpha}_{r(s)} + (n-\theta)\varepsilon^{\alpha}_{r(a)}, \tag{1}$$

where $\varepsilon_{r(w)}$ and $\varepsilon_{r(a)}$ are the dielectric permittivity of water (equal to 81) and air (equal to 1) respectively, $\varepsilon_{r(s)}$ is the relative dielectric permittivity of the soil particles, n is the porosity; θ is the volumetric soil water content and α is a factor accounting for the orientation of the electrical field.

[12] Figure 3 shows n for eight peat samples at different depths, as well as samples from the lake sediment and glaciomarine clay. The porosity of the peat varies from 91% to 94%. Assuming $\varepsilon_{r\ (peat)} = 2$ (as obtained from laboratory measurements) and $\alpha = 1$ for EM wave propagation parallel to bedding, in the absence of gas the CRIM model predicts v = 0.0346 m/ns to 0.0351 m/ns for 94% and 91% porosity respectively. These estimates are close to the lowest velocity of 0.0345 m/ns recorded between boreholes (Figure 2c).

4. Discussion

[13] The gas concentrations reported in this study are low when compared to concentrations reported for laboratory studies [e.g., *Baird and Waldron*, 2003] and for some field studies [e.g., *Dinel et al.*, 1988]. Although we cannot rule out potential contamination problems during the gas sampling procedure (i.e. atmospheric exposure), the results presented here are valid for comparative purposes.

[14] Application of the CRIM model (equation (1)) to the EM wave velocities obtained between boreholes implies that the anomalous high velocity zones result from significant volumetric gas content. To achieve the maximum velocities recorded (0.0365 m/ns) in the anomalous zones of Figure 2c the CRIM model predicts a volumetric gas content of 7% and 10% for a porosity of 91% and 94% respectively. In the absence of gas, the CRIM model predicts a porosity of only 84% in order to obtain the maximum velocity recorded between the boreholes. Such low porosity values are not supported by our data and are inconsistent with the high porosity of peat recorded by others. Figure 2c shows the estimated gas content (%) according to the CRIM model and assuming $\varepsilon_{r\ (peat)} = 2$, $\alpha = 1$, and a porosity of 0.94. These values are consistent with volumetric gas contents in peatlands estimated by others (e.g. 9% average gas using hydraulic head [*Rosenberry et al.*, 2003]).

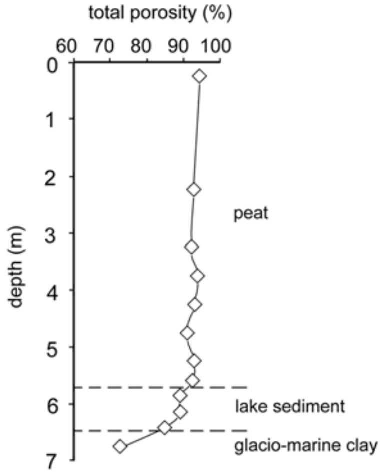

Figure 3. Total porosity (%) of eight peat samples, three lake sediment samples and one glacio-marine clay sample collected at variable depths at Caribou Bog.

[15] As shown in Figures 2b and 2c, shadow zones detected with surface GPR correlate with higher concentrations of CH_4 and CO_2, and with high velocity regions computed from the travel times between boreholes, being indicative of biogenic gas deposits. Figure 2a shows the location of the interpreted shadow zones according to the surface GPR. One of the characteristic features of these regions is the presence of strong, laterally continuous reflectors preceding the EM wave blanking as annotated in Figure 2a. These reflectors also coincide with EM wave velocity minimums in the ZOP. Three interpreted reflectors situated at 1.3 m, 3 m, and 4.5 m depth respectively correlate well with three velocity minimums (indicative of low gas content) at 1.4 m, 3 m and 4.8 m depth in Figure 2c. Figure 2a may represent overpressurized biogenic gas pockets contained by confining layers acting as biogenic gas traps as explained elsewhere [*Romanowicz et al.*, 1995; *Glaser et al.*, 2004]. The observed bubble release during piezometer installation as shown in Figure 2a may then result from disturbance of these layers during borehole installation. This model would partly explain the vertical distribution of averaged gas content between the boreholes as inferred from ZOP.

[16] We have obtained over 11 km of surface GPR data in Caribou Bog and we frequently observe zones of EM blanking that we attribute to gas deposits. Figure 4 shows two examples of GPR lines run in Caribou Bog. Figure 4a includes a clear example of reflector scattering (between 55–75 m along the profile) usually correlated with disappearance of single strong reflectors with depth. These shadow zones often correlate with a thickening of lake sediment where the peat basin deepens (Figure 4a). In contrast, Figure 4b shows mostly strong reflections along a profile where the mineral soil is at constant elevation. A small shadow zone can roughly be defined from 2–4 m depth between 0–25 m along the profile. Since no borehole GPR, gas sampling, or moisture probe data are available for

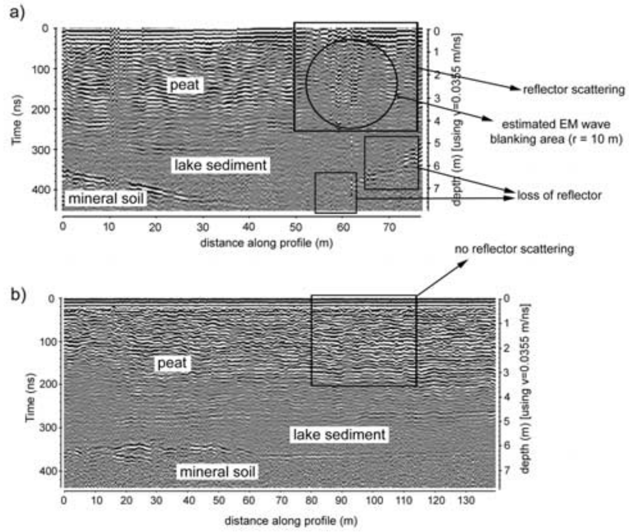

Figure 4. Surface GPR profiles collected in Caribou Bog showing (a) reflector scattering and loss of reflectors, and (b) absence of EM shadow zone. Stratigraphic units (in both Figure 4a and Figure 4b) and a circular estimated area affected by EM wave blanking for gas volume evaluation (in Figure 4a) are also shown.

these areas, correlation between such EM shadow zones and biogenic gas accumulation cannot be confirmed. However, and from the available hydrological and electrical measurements at Caribou Bog [e.g., *Comas et al.*, 2004], the uniformity of peat composition and pore fluid chemistry laterally, the slight variation in porosity (Figure 3), and the absence of surface structures that can generate scattering of the EM signal, point to the presence of gas as the most likely explanation for these shadow zones.

[17] A rough estimate of the amount of biogenic gas within a zone of EM wave blanking can be calculated. In Figure 4a, we estimate an affected circular area of 10 m radius (r) between 55 and 75 m distance along the profile. Assuming spherical volume and a maximum gas concentration 10%, a maximum gas content of 418,900 dm^3 is estimated. Considering the maximum biogenic gas concentrations obtained during sampling a total volume of 2,723 dm^3 of CH_4 and 2,095 dm^3 of CO_2 are estimated. This approach could be upscaled to estimate the total volume and variability of free gas in a peatland from a grid of GPR measurements over large scales. Furthermore, GPR monitoring might reveal information on the field-scale migration and release of biogenic gases in peatlands.

5. Conclusions

[18] We have shown that EM wave shadow zones (scattering of EM signal) recorded with surface GPR surveys correlate with areas of biogenic gas accumulation. Higher concentrations of CH_4 and CO_2 and increases in the EM wave velocity recorded in zero offset profiling between boreholes correlate with these shadow zones. The CRIM model is not applicable to the entire range of EM velocities obtained between the boreholes without accounting for the presence of gas up to 10% by volume. The presence of strong reflectors immediately above shadow zones may represent confining layers for gas traps as postulated by others. Spatial gas distribution and volumetric gas content can be estimated from the areas affected by EM wave blanking in surface GPR data. These findings also have implications for the monitoring of temporal behavior and variability of biogenic gas emissions to the atmosphere from peatlands.

[19] **Acknowledgments.** This material is based upon work supported by the National Science Foundation under Grant No. EAR-0242353. University of Maine graduate student Nathan Stevens provided valuable field support for which we extend our thanks. We also thank Andrew Baird and one anonymous reviewer for their suggestions to enhance the quality of an earlier version of this manuscript.

References

Baird, A. J., and S. Waldron (2003), Shallow horizontal groundwater flow in peatlands is reduced by bacteriogenic gas production, *Geophys. Res. Lett.*, *30*(20), 2043, doi:10.1029/2003GL018233.

Beckwith, C. W., and A. J. Baird (2001), Effect of biogenic gas bubbles on water flow through poorly decomposed blanket peat, *Water Resour. Res.*, *37*, 551–558.

Binley, A., P. Winship, R. Middleton, M. Pokar, and J. West (2001), High-resolution characterization of vadose zone dynamics using cross-borehole radar, *Water Resour. Res.*, *37*, 2639–2652.

Cicerone, R. J., and R. S. Oremland (1988), Biochemical aspects of atmospheric methane, *Global Biogeochem. Cycles*, *2*, 299–327.

Comas, X., L. Slater, and A. Reeve (2004), Geophysical evidence for peat basin morphology and stratigraphic controls on vegetation observed in a northern peatland, *J. Hydrol.*, *295*, 173–184.

Daniels, J. J., R. Roberts, and M. Vendl (1995), Ground penetrating radar for the detection of liquid contaminants, *J. Appl. Geophys.*, *33*, 195–207.

Dinel, H. S., S. P. Mathur, A. Brown, and M. Lévesque (1988), A field study of the effect of depth on methane production in peatland waters equipment and preliminary results, *J. Ecol.*, *76*, 1083–1091.

Fechner-Levy, E. J., and H. F. Hemond (1996), Trapped methane volume and potential effects on methane ebullition in a northern peatland, *Limnol. Oceanogr.*, *41*, 1375–1383.

Glaser, P. H., P. J. Morin, J. Kamp, N. Tsekos, and D. I. Siegel (1998), Measuring biogenic-gas bubbles in peat cores by magnetic resonance imaging, *Eos Trans. AGU*, *79*(17), Spring Meet. Suppl., Abstract A51B-3.

Glaser, P. H., J. P. Chanton, P. Morin, D. O. Rosenberry, D. I. Siegel, O. Ruud, L. I. Chasar, and A. S. Reeve (2004), Surface deformations as indicators of deep ebullition fluxes in a large northern peatland, *Global Biogeochem. Cycles*, *18*, GB1003, doi:10.1029/2003GB002069.

Huisman, J. A., S. S. Hubbard, J. D. Redman, and A. P. Annan (2003), Measuring soil water content with ground penetrating radar: A review, *Vadoze Zone J.*, *2*, 476–491.

Judd, A. G., and M. Hovland (1992), The evidence of shallow gas in marine sediments, *Cont. Shelf Res.*, *12*, 1081–1095.

Khalil, M. A. K. (2000), *Atmospheric Methane: Its Role in the Global Environment*, Springer, New York.

Landva, A. O., and P. E. Pheeney (1980), Peat fabric and structure, *Can. Geotech. J.*, *17*, 416–435.

Lopes de Castro, D., and R. M. G. C. Branco (2003), 4-D ground penetrating radar monitoring of a hydrocarbon leakage site in Fortaleza (Brasil) during its remediation process: A case history, *J. Appl. Geophys.*, *54*, 127–144.

Price, J. S. (2003), Role and character of seasonal peat soil deformation on the hydrology of undisturbed and cutover peatlands, *Water Resour. Res.*, *39*(9), 1241, doi:10.1029/2002WR001302.

Romanowicz, E. A., D. I. Siegel, J. P. Chanton, and P. H. Glaser (1995), Temporal variations in dissolved methane deep in the Lake Agassiz peatlands, Minnesota, *Global Biogeochem. Cycles*, *9*, 197–212.

Rosenberry, D. O., P. H. Glaser, D. I. Siegel, and E. P. Weeks (2003), Use of hydraulic head to estimate volumetric gas content and ebullition flux in northern peatlands, *Water Resour. Res.*, *39*(3), 1066, doi:10.1029/2002WR001377.

Roulet, N. T., R. Ash, W. Quinton, and T. Moore (1993), Methane flux from drained northern peatlands: Effect of a persistent water table lowering on flux, *Global Biogeochem. Cycles*, *7*, 749–770.

X. Comas and L. Slater, Department of Earth and Environmental Sciences, Rutgers University, Newark, NJ 07102, USA. (xcomas@pegasus.rutgers.edu; lslater@andromeda.rutgers.edu)

A. Reeve, Department of Earth Sciences, University of Maine, Orono, ME 04469, USA. (asreeve@maine.edu)